

Supporting information

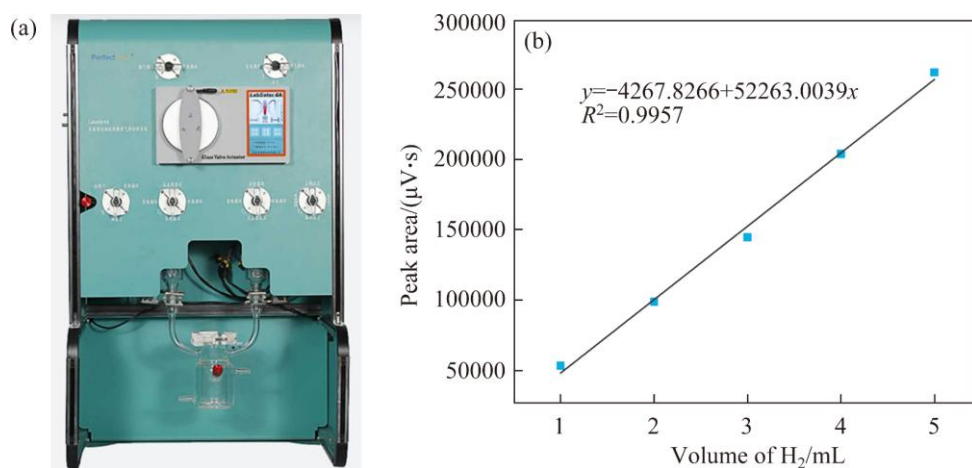


Figure S1 (a) Photocatalytic all-glass closed gas system (Labsolar-6A, PerfectLight); (b) Calibration curve of photocatalytic H_2 evolution

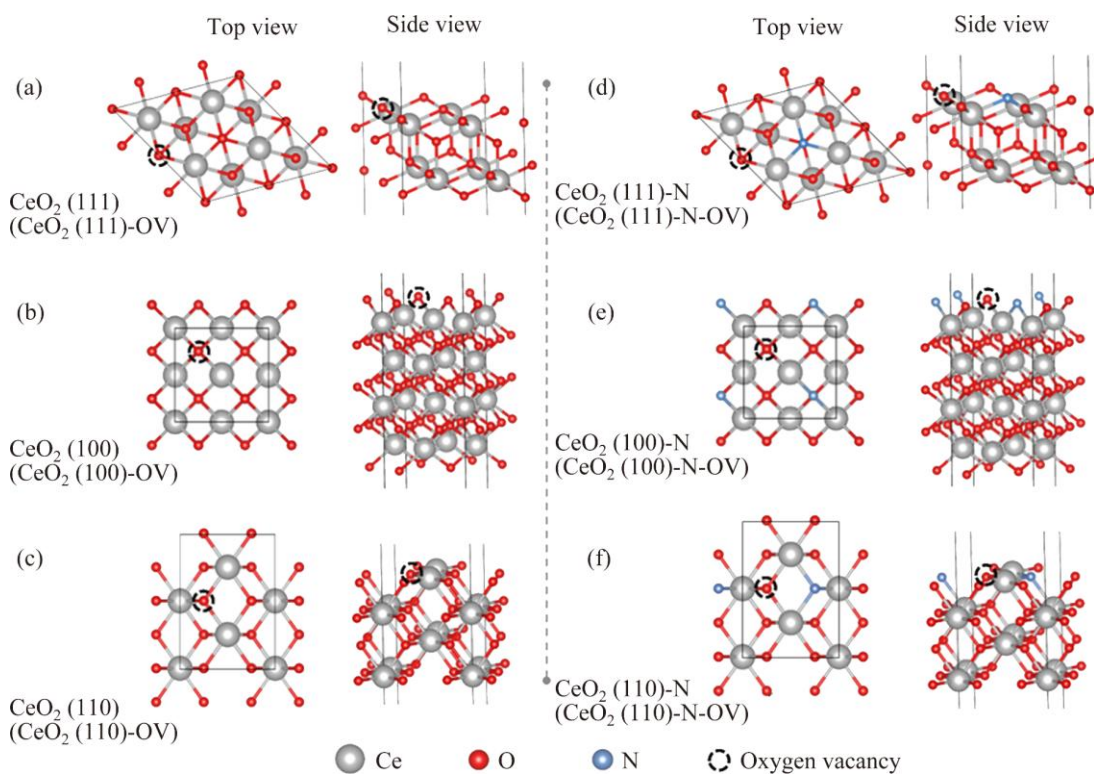


Figure S2 The top and side views of constructed CeO_2 (111), (100), and (110) surfaces

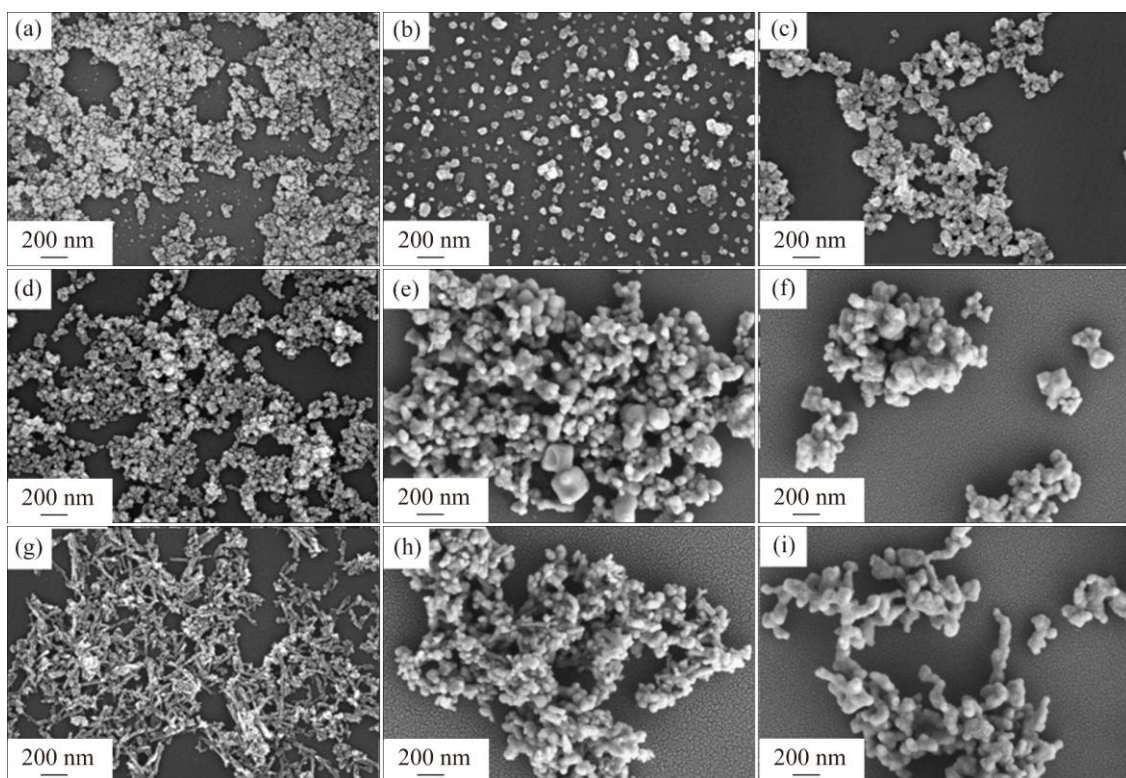


Figure S3 SEM images of P-CeO₂ (a), P-CeO₂-N₂ (b), and P-CeO₂-NH₃ (c), C-CeO₂ (d), C-CeO₂-N₂ (e), and C-CeO₂-NH₃ (f), R-CeO₂ (g), R-CeO₂-N₂ (h), and R-CeO₂-NH₃ (i)

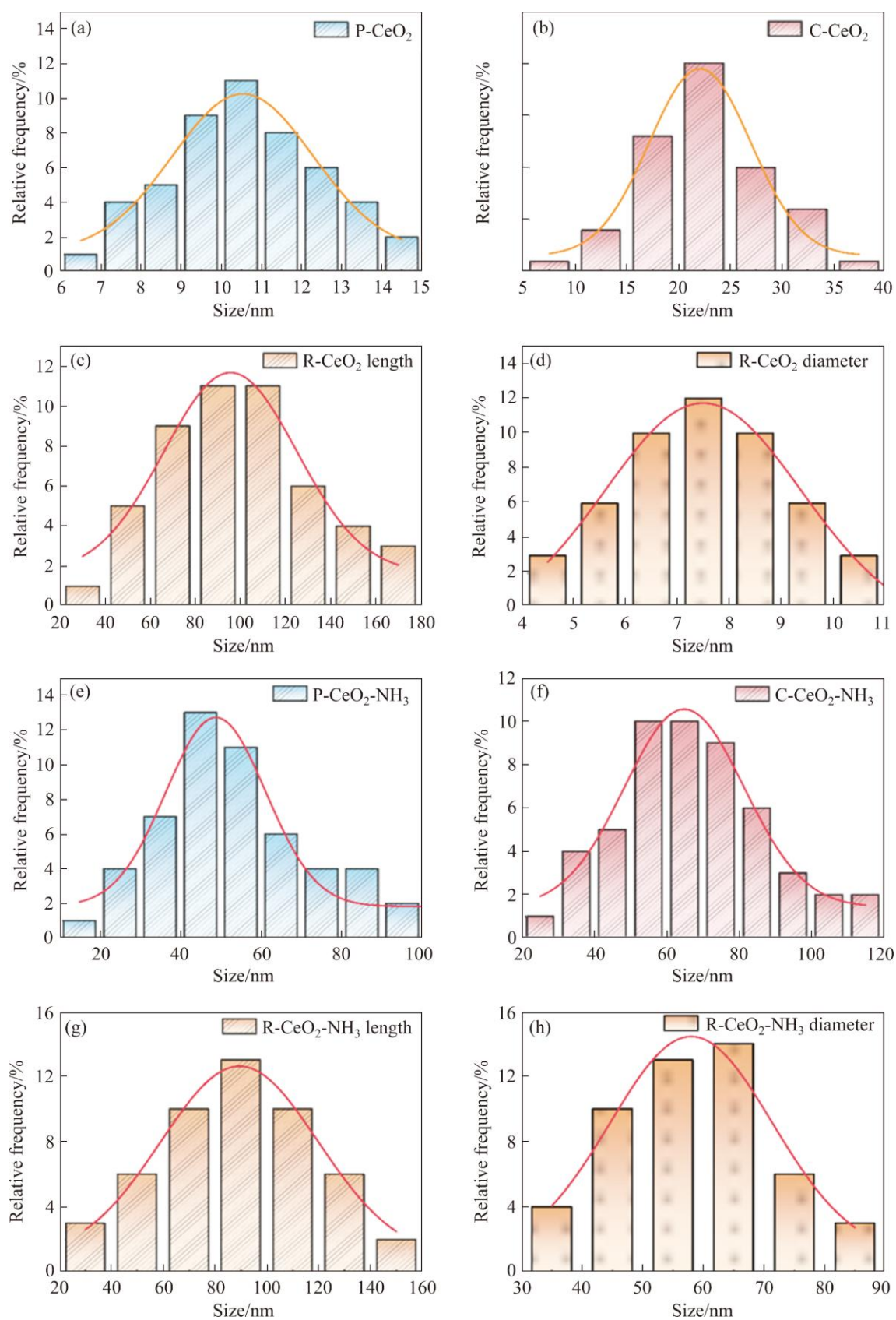


Figure S4 Particle size distribution of P-CeO₂ (a), C-CeO₂ (b), R-CeO₂ (c, d), P-CeO₂-NH₃ (e), C-CeO₂-NH₃ (f), and R-CeO₂-NH₃ (g, h)

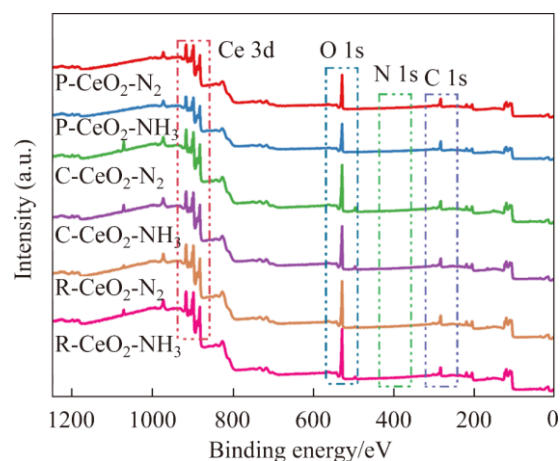


Figure S5 XPS spectra of prepared CeO₂

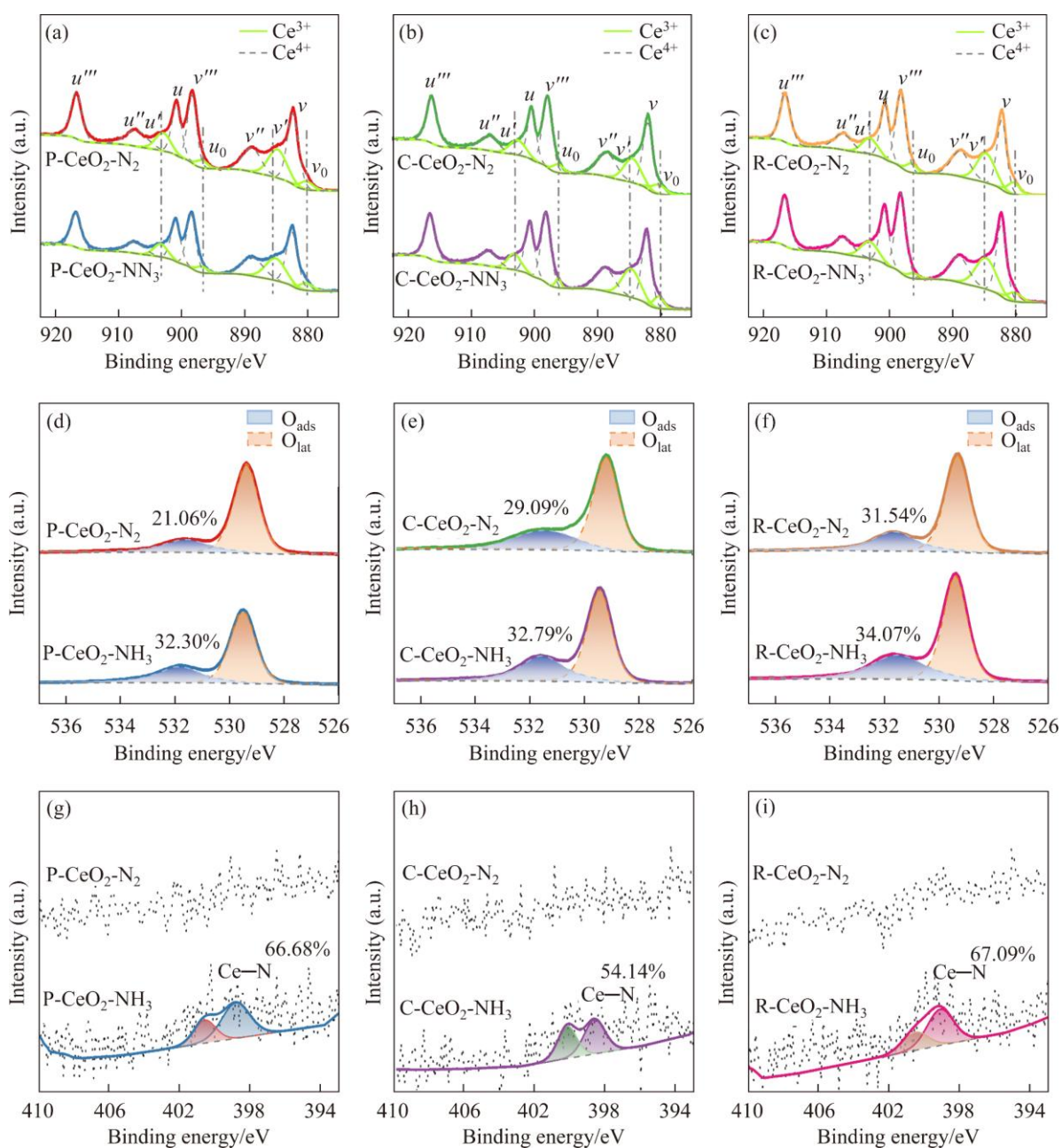


Figure S6 XPS results of the Ce 3d (a-c), O 1s (d-f), and N 1s (g-i) of N-doped CeO₂

The percentage of Ce^{3+} and O_{ads} can be calculated by the following formula [1]:

$$C_{\text{Ce}^{3+}} = \frac{\text{Peak area}(v_0, u_0, v', u')}{\text{Total peak area}} \times 100\%$$

$$C_{\text{O}_{\text{ads}}} = \frac{\text{Peak area}(\text{O}_{\text{ads}})}{\text{Total peak area}} \times 100\%$$

$$C_{(\text{Ce-N})} = \frac{\text{Peak area}(\text{Ce-N})}{\text{Total peak area}} \times 100\%$$

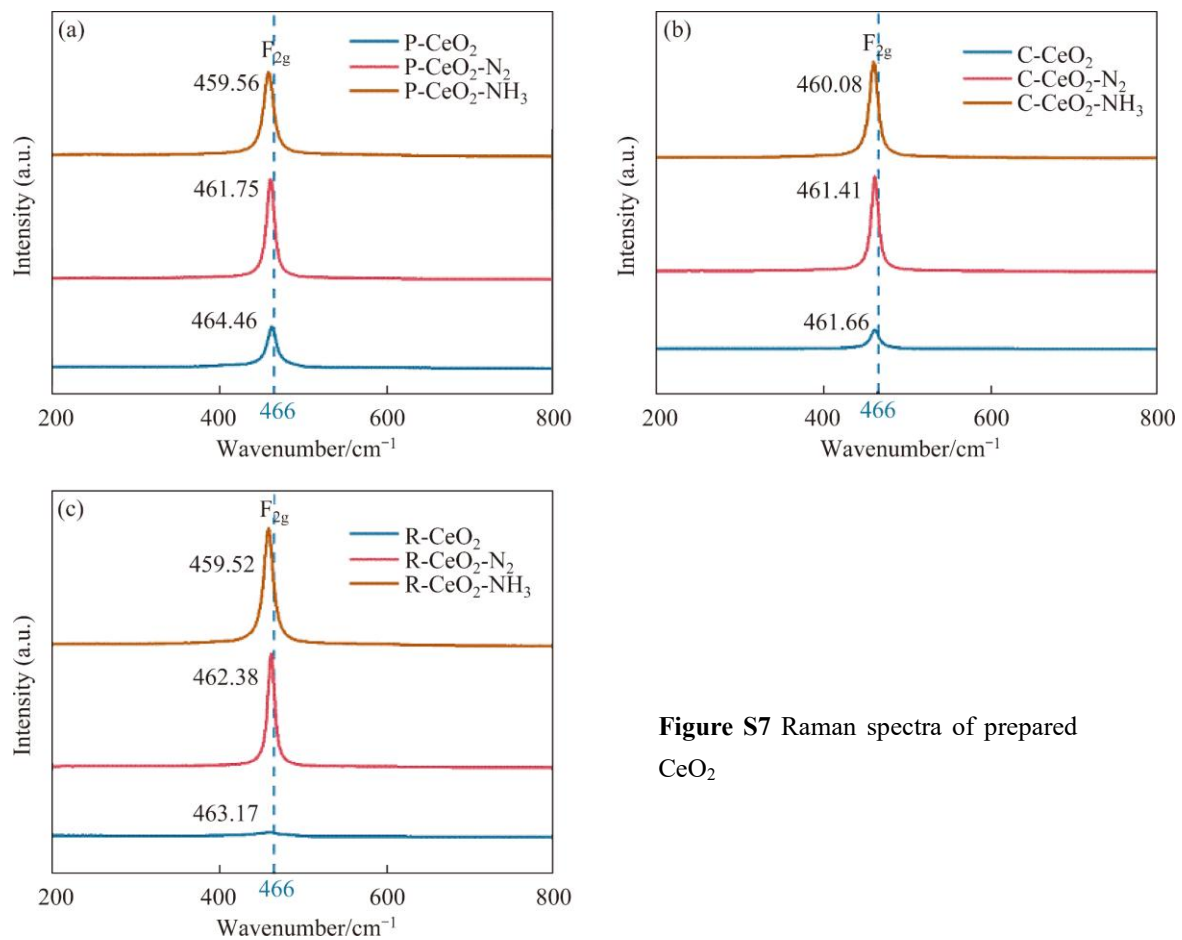


Figure S7 Raman spectra of prepared CeO_2

Due to the low concentration of the organic solution and weak adsorption, the photocatalytic kinetics followed the Langmuir-Hinshelwood model (L-H model) is [2]:

$$\ln \frac{c_0}{c} = kt$$

where k is the apparent rate constant, and t is the photocatalytic reaction time.

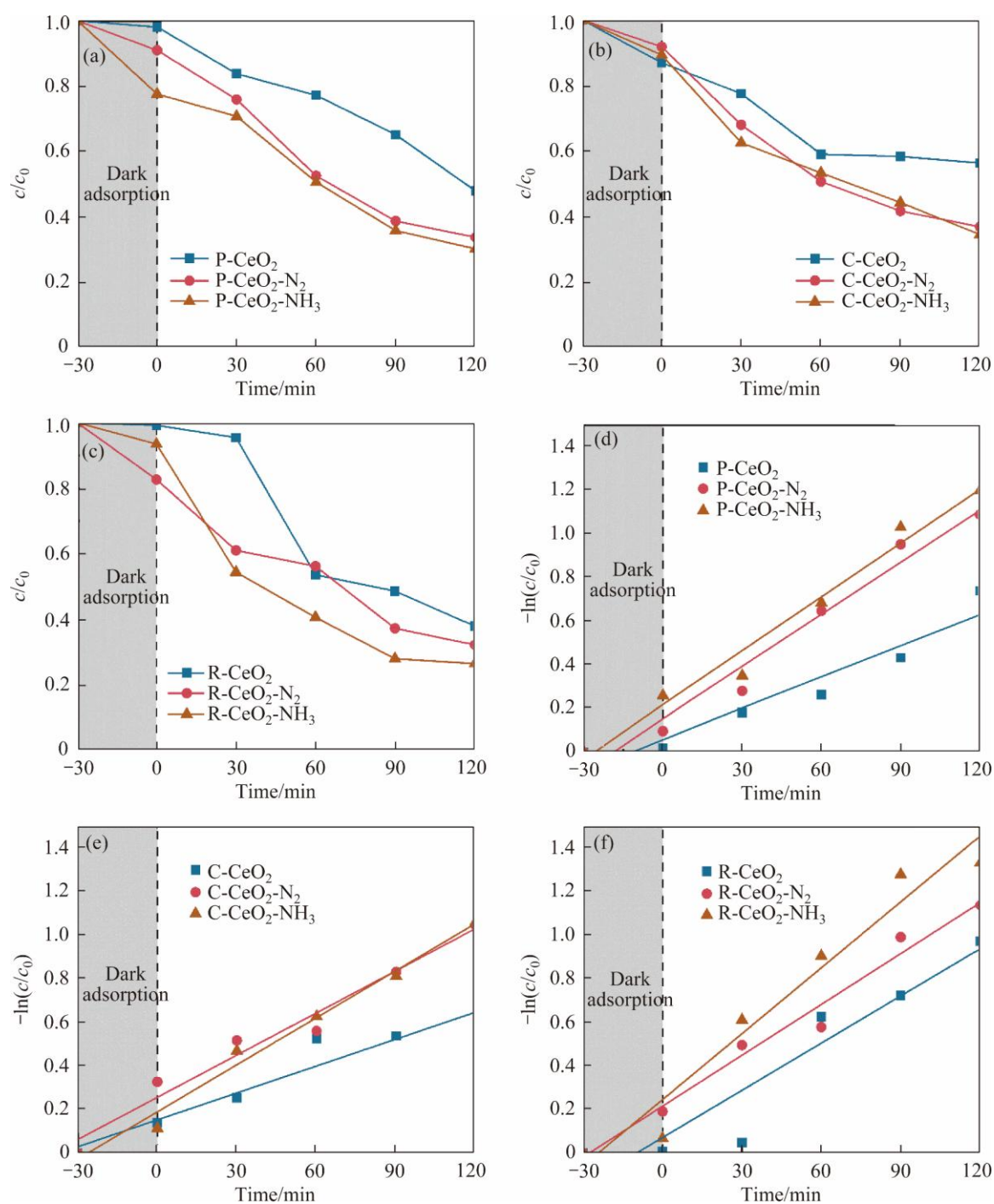


Figure S8 The photodegradation efficiency (c/c_0) and the fitted kinetics curves of TC by prepared CeO_2

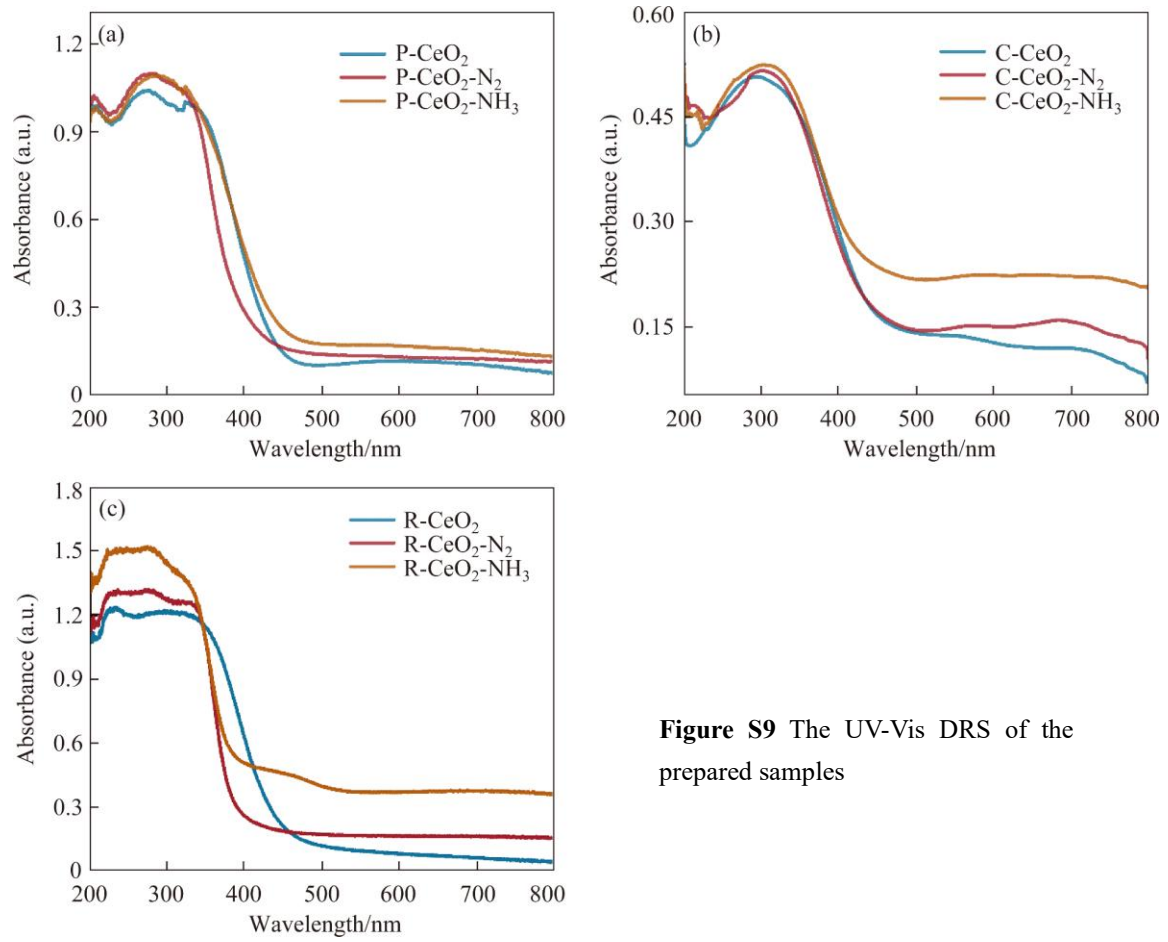


Figure S9 The UV-Vis DRS of the prepared samples

The band gap is calculated by Tauc's formula [3]:

$$(\alpha h\nu)^n = A(h\nu - E_g)$$

where α , h , ν , A and E_g represent the absorption coefficient, Planck's constant, photon frequency, proportionality constant, and band gap of a semiconductor, respectively, and the value of n for CeO_2 with a direct band gap is 2 [4].

Then, the valence band (E_{vb}) can be calculated by formula:

$$E_{vb} = E_{cb} + E_g$$

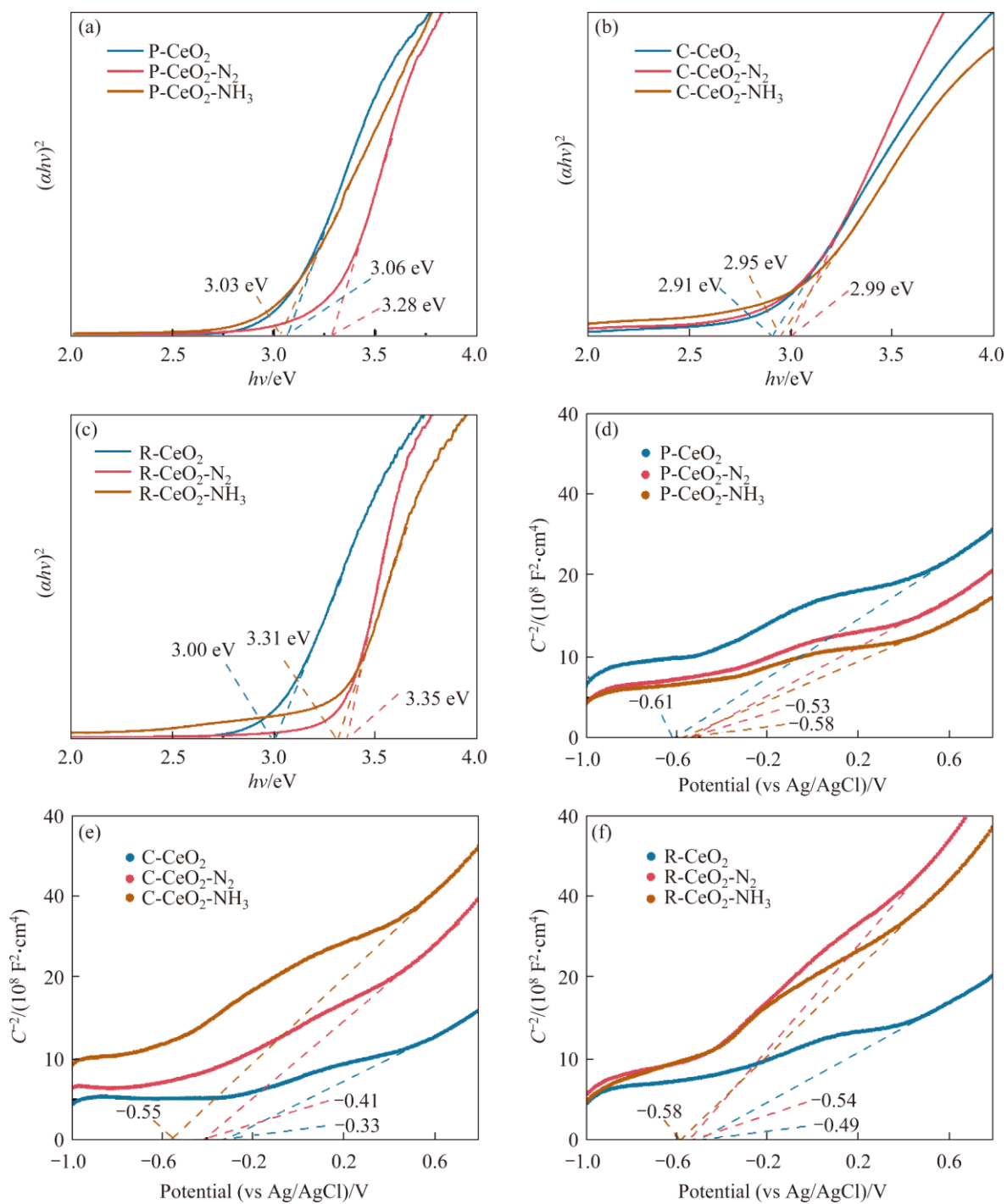


Figure S10 The Kubelka-Munk plots (a–c) and Mott-Schottky plots (d–f) of the prepared samples (C is the electric capacity)

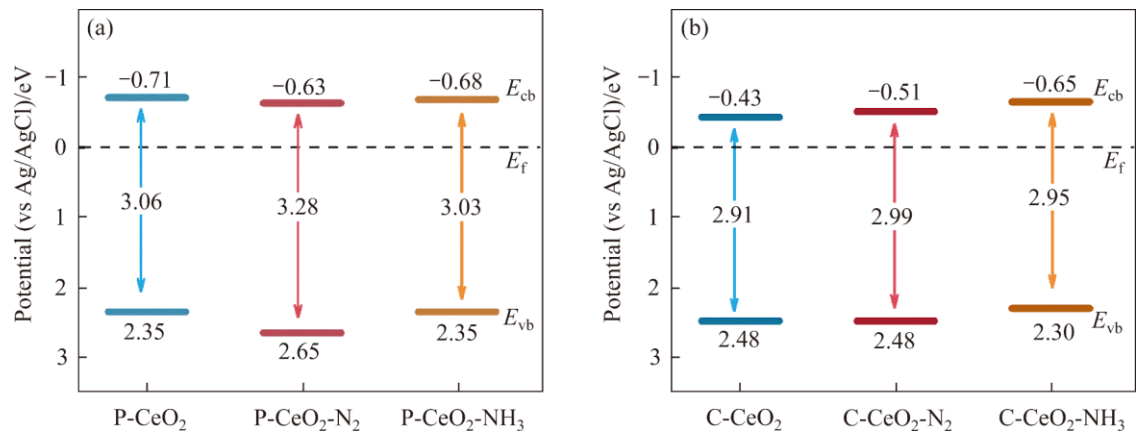


Figure S11 The potential diagrams of band structures of P-CeO₂ (a) and C-CeO₂ (b) systems

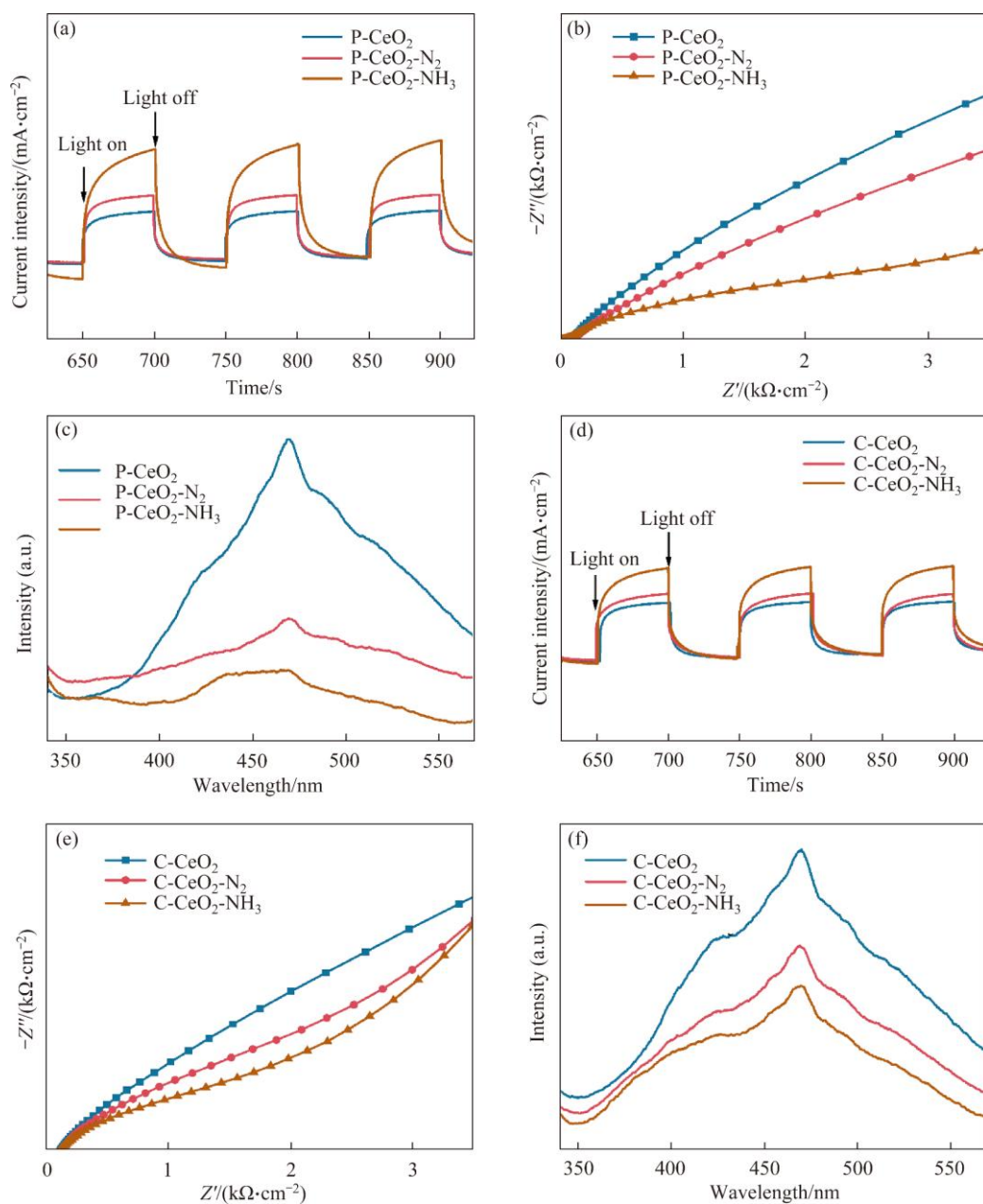


Figure S12 The photocurrent curves (a and d), impedance spectra (b and e), and PL spectra (c and f) of samples

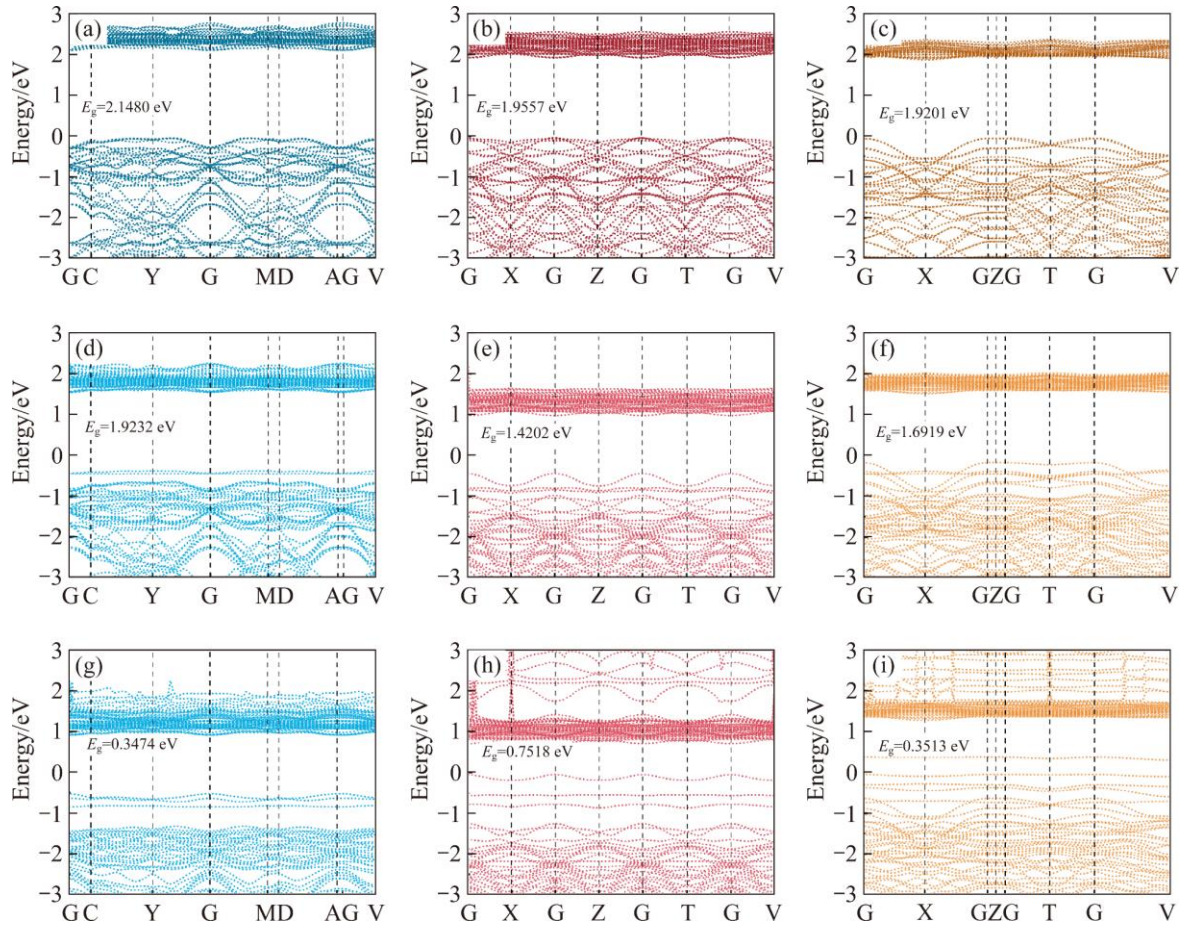


Figure S13 Band structures of CeO₂ (111) (a), CeO₂ (100) (b), CeO₂ (110) (c), CeO₂ (111)-N (d), CeO₂ (100)-N (e), CeO₂ (110)-N (f), CeO₂ (111)-N-OV (g), CeO₂ (100)-N-OV (h), CeO₂ (110)-N-OV (i)

Table S1 The calculated Ce³⁺, O_{ads} and Ce-N contents of XPS results

| Sample | cCe3+/% | cOads/% | cCe-N/% |
|-------------------------------------|---------|---------|---------|
| P-CeO ₂ -N ₂ | 23.48 | 21.06 | — |
| P-CeO ₂ -NH ₃ | 24.35 | 32.30 | 66.68 |
| C-CeO ₂ -N ₂ | 22.30 | 29.09 | — |
| C-CeO ₂ -NH ₃ | 23.33 | 32.79 | 54.14 |
| R-CeO ₂ -N ₂ | 24.30 | 31.54 | — |
| R-CeO ₂ -NH ₃ | 25.08 | 34.07 | 67.09 |

Table S2 The DFT calculated energy of surface models and formation energy of the doped system

| Sample | $E_{\text{surf-N}}/\text{eV}$ | $E_{\text{surf}}/\text{eV}$ | E_{O}/eV | E_{N}/eV | $E_{\text{form}}/\text{eV}$ |
|------------------------|-------------------------------|-----------------------------|--------------------------|--------------------------|-----------------------------|
| CeO ₂ (111) | -189.8195 | -191.7122 | | | 3.2857 |
| CeO ₂ (100) | -188.4499 | -190.2218 | -1.6278 | -3.0208 | 3.1649 |
| CeO ₂ (110) | -189.0781 | -190.8074 | | | 3.1223 |

Table S3 The DFT calculated energy of surface models and formation energy of oxygen vacancy

| Sample | $E_{\text{surf}}/\text{eV}$ | $E_{\text{surf-OV}}/\text{eV}$ | $\frac{1}{2}E_{\text{O}_2}/\text{eV}$ | E_{OV}/eV |
|--------------------------|-----------------------------|--------------------------------|---------------------------------------|---------------------------|
| CeO ₂ (111) | -191.7122 | -184.8496 | -4.8893 | 1.9733 |
| CeO ₂ (111)-N | -189.8195 | -183.3776 | | 1.5526 |
| CeO ₂ (100) | -190.2218 | -183.4457 | | 1.8868 |
| CeO ₂ (100)-N | -188.4499 | -182.0358 | | 1.5248 |
| CeO ₂ (110) | -190.8074 | -183.8746 | | 2.0435 |
| CeO ₂ (110)-N | -189.0781 | -182.7026 | | 1.4862 |

References

- [1] WANG Fan, LI Jun-qi, CHEN Chao-yi, et al. Enhancement effects of surface and bulk oxygen vacancies on the photocatalytic properties of ceria [J]. *Molecular Catalysis*, 2023, 549: 113507. DOI: 10.1016/j.mcat.2023.113507.
- [2] LIU Bao-shun, ZHAO Xiu-jian, TERASHIMA C, et al. Thermodynamic and kinetic analysis of heterogeneous photocatalysis for semiconductor systems [J]. *Physical Chemistry Chemical Physics*, 2014, 16(19): 8751–8760. DOI: 10.1039/c3cp55317e.
- [3] ABOU EL-ENEIN S A, ALI A M, ABDEL-MONEM Y K, et al. Novel lanthanide(III) 4-methylbenzoylhydrazide complexes as precursors for lanthanide oxide nanophotocatalysts [J]. *RSC Advances*, 2019, 9(72): 42010–42019. DOI: 10.1039/c9ra08080e.
- [4] YASHODHA S R, DHANANJAYA N, MANJUNATH C. Synthesis and photoluminescence properties of Sm³⁺ doped LaOCl phosphor with reddish orange emission and its Judd-Ofelt analysis [J]. *Materials Research Express*, 2020, 7(1): 015003. DOI: 10.1088/2053-1591/ab57a6.